LIDAR based distance estimation for emergency use terrestrial autonomous robot

2021 13th International Conference on Electronics, Computers and Artificial Intelligence (ECAI) | 978-1-6654-2534-6/21/$31.00 ©2021 IEEE | DOI: 10.1109/ECAI52376.2021.9515047

1st Răzvan-Ionuț BĂLAȘA
Faculty of Integrated Armed Systems, Engineering and Mechatronics
Military Technical Academy FERDINAND I
Bucharest, Romania
razvan.balasa@mta.ro

2nd Ghoerghe OLARU
Faculty of Integrated Armed Systems, Engineering and Mechatronics
Military Technical Academy FERDINAND I
Bucharest, Romania
gheorghe.olaru@mta.ro

3rd Daniel CONSTANTIN
Faculty of Integrated Armed Systems, Engineering and Mechatronics
Military Technical Academy FERDINAND I
Bucharest, Romania
daniel.constantin@mta.ro

4th Amado ȘTEFAN
Faculty of Aircraft and Military Vehicles, Department of Integrated Aviation and Mechanical Systems
Military Technical Academy FERDINAND I
Bucharest, Romania
amado.stefan@mta.ro

5th Ciprian-Marian BÎLU
I.N.C.A.S. - National Institute for Aerospace Research "Elie Carafoli"
Bucharest, Romania
bilu.ciprian@incas.ro

6th Maria Beatrice BĂLĂCEANU
Panda Bears Technologies S.R.L.
Bucharest, Romania
bmariabeatrice@yahoo.com

***Abstract* — In this research we have proposed the implementation of a Lio-Sam algorithm in the navigation system of an autonomous terrestrial robot. This algorithm is based on the following sensors: Ouster OS1-64 Light Detection and Ranging device (LIDAR) and an XSens MTI 1 Inertial Measurement Unit (IMU). We have opted for this algorithm due to the fact that for the swarm and emergency intervention robots it constitutes a very good solution, especially because it can help us generate a 3D point cloud map of the surroundings. The significant advantage of this solution is that it allows a fast identification of the location of the robot.**

Keywords — robot, LIDAR, autonomous, testing, emergency

I. Introduction

One of the most difficult tasks a rover must perform while navigating towards either a pre-defined or mobile target is collision avoidance [1,2]. Some of the main disadvantages of the navigation system of a terrestrial robot are linked to the equipment responsible of image acquisition and processing, namely the illumination conditions, reflections, shadows, movement distortions and sensors field of view [3-5].

This is the reason why we consider that a sensors system based on LIDAR not only can significantly improve the chances to identify an obstacle in the robot's path, but it can also help reconstruct the 3D map of the environment in which it moves [6,7].

Another significant advantage of this technology is that the orientation of the objects does not introduce additional errors in computing the minimum distance between the rover and the obstacle. Moreover, it offers us the possibility to compute the distance between two points from different objects or from two points of the same object, which could lead to a better decision for the optimal path which we want our rover to follow [8-11].

In order for LIOSAM (Lidar Inertial Odometry via Smoothing and Mapping), the computational algorithm, to be able to re-create the virtual map as precisely as possible under the conditions of a sudden LIDAR movement, we will need an IMU sensor whose information helps reconstruct the real image [12,13].

II. Related Work

Using the LIDAR involves working with the notion of LIDAR odometry. This principle uses scanning and matching between two consecutive frames [14,15], thus the methods become simpler, without the need to match the data with a complete cloud. In order to extract the planes from the 3D point maps and to match them, we are using a strategy for minimizing the error, namely the least square errors method. We can state that the real-time LIDAR odometry is an efficient approach.

In order to estimate the position, the sole use of the LIDAR sensor is not enough because recording the data based on the point cloud information does not define the absolute orientation characteristics of the objects. This is the reason why the LIDAR has to be used together with the XSens MTI 1 sensor for now. In the future we will also introduce data from a GPS sensor too in order to improve the mapping process. In order to represent the state vector of the robot ("ROV"), we need to define W as "world frame", and B as "robot body frame". Thus. the following equation can be used [16]:

$$\mathrm{ROV} = \left[R^T, p^T, v^T, b^T \right]^T \tag{1}$$

where: $R \in SO(3)$ - the rotation matrix; $p \in \mathbb{R}^3$ – the position vector, $v\left[m/s \right]$ - the velocity of the robot; **b** is the IMU bias.

In order to determine the state vector of the robot at any given time and reconstruct its trajectory, the data from the LIDAR and the IMU is used. The problem of estimating the state can be estimated as a Maximum a Posteriori Problem (MAP), because using a factorial graph for checking the inferences is more suitable than using Bayesian networks.

978-1-6654-2534-6/20/$31.00 ©2020 IEEE

Authorized licensed use limited to: Otto-von-Guericke Universitaet Magdeburg. Downloaded on September 11,2022 at 14:08:34 UTC from IEEE Xplore. Restrictions apply.

The MAP inference helps solve a nonlinear problem by using the least square method.

A new computational method introduces new factors together with a variable type for building the graph of the factors. The variable represents the state of the robot at a given moment, representing each graph node. Among the numerous integration elements, we mention: IMU, LIDAR odometry elements and closed loop factors.

A. IMU Preintegration Factor

Applying the IMU pre-integration method ([16], [17]) in order to determine the relative movement of the body between two steps uses the pre-integrated measurements Δv_{ij}, Δp_{ij} and ΔR_{ij} between time i and time j as follows:

$$\Delta v_{ij} = R_i^T \left(v_j - v_i - g\Delta t_{ij} \right) \tag{2}$$

$$\Delta p_{ij} = R_i^T \left(p_j - p_i - v_i \Delta t_{ij} - \frac{1}{2} g \Delta t_{ij}^2 \right) \tag{3}$$

$$\Delta R_{ij} = R_i^T \cdot R_j \tag{4}$$

B. LiDAR Odometry Factor

For each LIDAR scan, the extraction of the marginal and planar features will be performed by verifying the points rugosity over a given region ([18]). The high rugosity points are classified as edge features, while a low rugosity value indicates a planar feature.

All the extracted features at a given moment make up an Fi LIDAR frame, where $F_i = \left\{ F_i^e, F_i^p \right\}$. Adding key frames helps balance the point map density with the storage consumption, while keeping a small factors graph. This aids the real-time non-linear optimization. The real-time odometry factor can be computed by using the following equations:

$$\begin{cases} M_i = \left\{ M_i^e, M_i^p \right\} \\ M_i^e = F_i^e \bigcup F_{i-1}^e \bigcup \ldots \bigcup F_{i-n}^e \\ M_i^p = F_i^p \bigcup F_{i-1}^p \bigcup \ldots \bigcup F_{i-n}^p \end{cases} \tag{5}$$

III. Framework Overview

Thus, in order to reconstruct the shape of various potential elements surrounding the path on which the rover moves, a LIDAR Ouster OS1-64 has been used together with a XSens MTI 1 IMU. These objects are represented as 3D point-clouds, which allows us to compute the distance between two points in order to enhance our collision avoidance capability. For example, our robot might be in front of a corridor, here the IR distance sensors do not detect an obstacle, but we want to check if the robot fits through this corridor (especially if, later on, it narrows). The data fusion algorithm which has been applied is LIO-SAM, referenced in [18]. LIO-SAM uses a non-linear movement model in order to de-skew the point cloud obtained from the LIDAR. The first step in estimating the trajectory consists of this algorithm using raw IMU measurements.

After the IMU data is applied for the point cloud de-skewing, the resulted enhanced LIDAR odometry is used in order to check for and correct an IMU bias. In this implementation, only measurements from the LIDAR and the IMU have been used. however, the performance of the algorithm can be increased by using GPS data

IV. Results for the 3D LIDAR Mapping

A. Characterization of the environment

This system has been tested both outside (in an open space area) and inside (in a Mechatronics laboratory).

It should be noted that, the algorithm has been applied in the post-processing step because the graphical processor of the on-board computer with which the measurements have been taken wasn't enough to ensure the real time operation with both measurement acquisition and data fusion.

If an on-board computer with higher graphics capabilities is used, the data fusion algorithm can be run after each measurement step.

In order to enhance the 3D points distance estimation accuracy, a 3.38 cm correction has been performed.

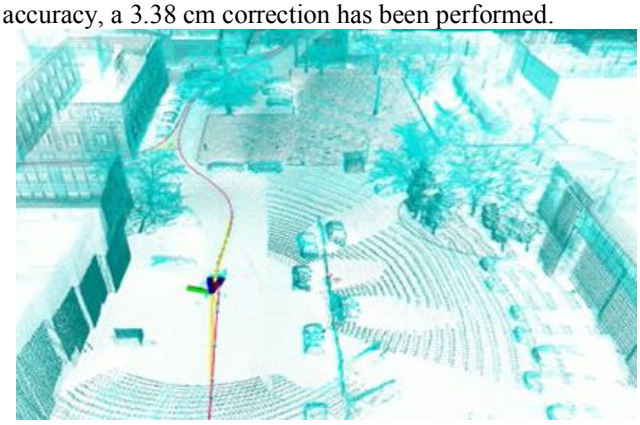

Fig. 1. Environment reconstruction and robot path estimation using Lio Sam (front view).

In case the algorithm runs in real-time (after each measurement step), the needed correction can be computed at system initialization (either manually by the user or autonomously by using a laser sensor) and then applied after the algorithm has finished running.

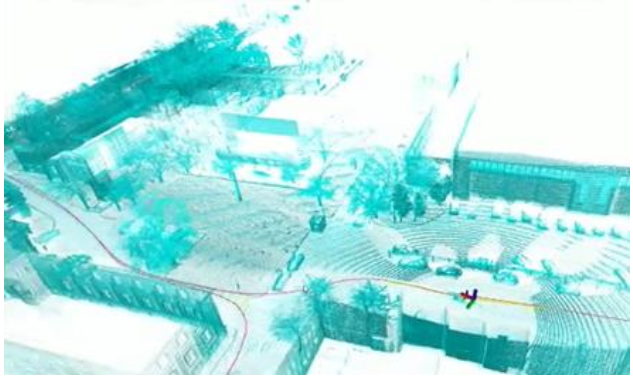

Fig. 2. Environment reconstruction and robot path estimation using Lio Sam (side view).

The performance of the system can be considered satisfactory since the objects with large dimensions have been well reconstructed, the trajectory has been estimated correctly and even details (such as leaves from trees or car components) have been rendered "Fig. 1." and "Fig. 2."

Authorized licensed use limited to: Otto-von-Guericke Universitaet Magdeburg. Downloaded on September 11,2022 at 14:08:34 UTC from IEEE Xplore. Restrictions apply.

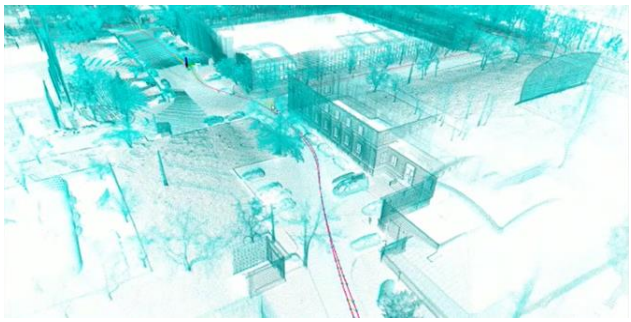

Fig. 3. Environment reconstruction and robot path estimation using Lio Sam (extended view).

The major advantage of the point cloud approach for special intervention rovers is that after an area is fully mapped by a drone or robot, another robot can use this data in order to navigate the surroundings "Fig. 3.". In this sense, the new robot which passes though the same path can scan only a part of a large building and, by using a mobile window approach, identify which portion of the map that part corresponds to. This could be useful in the case of robots which have to move in a known (previously mapped) area, such as fire-fighter robots, emergency use robots ([19]) and even robots which have to deliver and operate equipment in disaster areas.

B. Distance estimation

One example of a possible situation when a rover has to enter a narrow corridor can be found in the following figure, where a laboratory is mapped, and the width of a hallway entrance is measured "Fig. 4.":

Fig. 4. 3D point cloud rendering of a laboratory (the width of the hallway entrance is marked with the black line).

The distance estimation algorithm has been applied for various objects with different shapes. The most representative results for the distance estimation are the following "Fig. 5.".

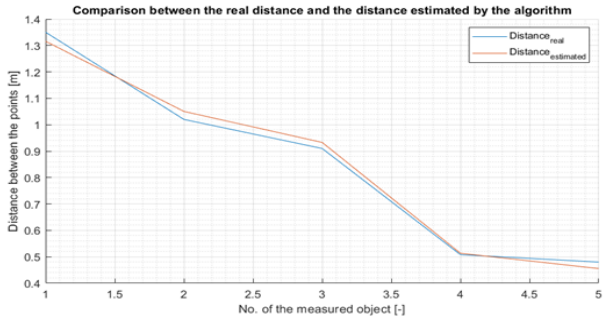

Fig. 5. Comparison between the estimation distance and the real distance.

The absolute error of the real distance between the two points and the estimated distance is represented in "Fig. 6.".

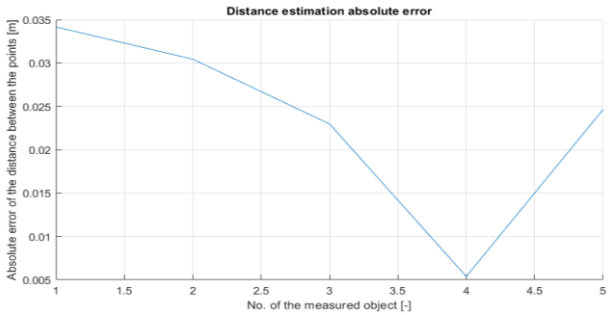

Fig. 6. Absolute error for the estimated distance.

As it can be noted, the absolute error is way below the 25 cm threshold for which the robot stops when encountering an obstacle ("Fig. 6."). Moreover, this small error can help validate the 3D reconstruction of the objects via the point cloud. This means that the resulting 3D map can be used for trajectory optimization (in order to save energy and fuel and avoid possible threats from the environment such as potholes or obstacles that might make the robot trip or flip over).
The relative error of the real distance between the two points and the estimated distance is represented in "Fig. 7.".

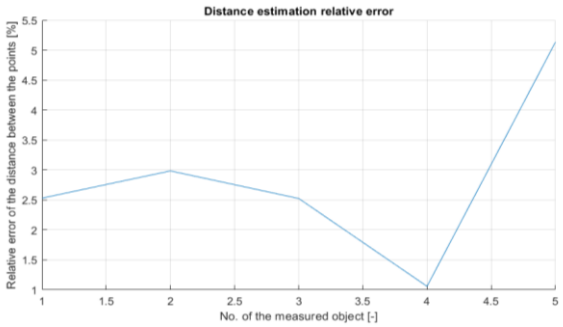

Fig. 7. Relative error for the estimated distance.

It should be noted that the highest relative error corresponds to the objects which are the farthest from the LIDAR and also have a small dimension (~0.488 m). The lowest relative error corresponds to objects which are close to the LIDAR.

These results indicate the fact that the rover is able to estimate distances and manage to avoid eventual collisions with different objects regardless of their size or shape. For example, the image below represents a measurement taken from a wing cross-sectional area "Fig. 8.".

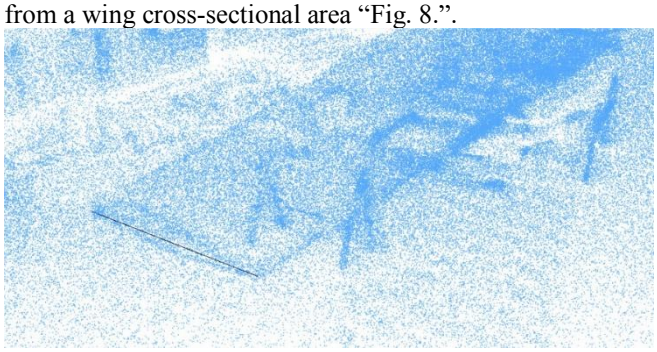

Fig. 8. Wing cross-sectional area - leading edge to trailing edge distance estimation.

V. Conclusion

In conclusion, the system behaves well regardless of the illumination and weather conditions. Moreover, it manages to

Authorized licensed use limited to: Otto-von-Guericke Universitaet Magdeburg. Downloaded on September 11,2022 at 14:08:34 UTC from IEEE Xplore. Restrictions apply.

map the 3D objects with high fidelity and to estimate the distances from two different points with an accuracy of several centimeters which is more than sufficient for our rover. Upon encountering an obstacle, our rover has to stop at 25 cm from it, while the maximum error has been less than 3.5 cm. This is also a promising result for the possibility of optimizing the trajectories of other rovers which have to go through the same environment and have the point cloud information from our rover.

ACKNOWLEDGMENT

This study has benefited from material support, scientific consulting, and it has been used through the project with the following title: "UAV Platform (unmanned aerial vehicles) with dedicated capabilities and support infrastructure, for applications in national security missions" mentioned in [20]. All the necessary equipment has been purchased in this project. We would like to thank the National Institute of Aerospace Research and Development "Elie Carafoli" and especially the chief of the Systems department, Dragoș Daniel Ion Guță, who allowed us to use the equipment needed to perform the tests.

We would also like to thank the Center of Excellence in Robotics and Autonomous Systems – CERAS for supporting us in the continuation of the research activities.

REFERENCES

[1] L.Ș. Grigore, I. Priescu, and D.L. Grecu, *Inteligența Artificială Aplicată în Sisteme Robotizate Fixe și Mobile*, Ed. AGIR, ISBN: 978-973-720-767-8, Street Calea Victoriei, no. 118, Bucharest, code 010093, pp. 683.

[2] L.Ș. Grigore, I. Priescu, D. Joița and Holban-Oncioiu I., "The Integration of Collaborative Robot Systems and Their Environmental Impacts", *MDPI, Processes*, ISSN: 2227-9717, Vol. 8, issue 4, 494, pp. 11, 21 April 2020.

[3] C. Ye, J. Borenstein, A new terrain mapping method for mobile robot's obstacle negotiation. *In Proceedings of the Unmanned Ground Vehicle Technology*, Orlando, FL, USA, 30 September 2003; pp. 52–63.

[4] N. Zhang, Yongjia Zhao, Fast and Robust Monocular Visua-Inertial Odometry Using Points and Lines, Sensors (Basel) 2019 Oct; 19(20): 4545, Published online 2019 Oct 19, doi: 10.3390/s19204545.

[5] E.A.K. Cohen, A.V. Abraham, S. Ramakrishnan, *et al.* Resolution limit of image analysis algorithms. *Nat Commun* 10, 793 (2019). https://doi.org/10.1038/s41467-019-08689-x.

[6] G. Zaidner, A. Shapiro - "A novel data fusion algorithm for low-cost localisation and navigation of autonomous vineyard sprayer robots", Biosystems Engineering 2016, ISSN: 1537-5110, Special Issue: Advances in Robotic Agriculture for Crops, 146, pp. 133-148 https://doi.org/10.1016/j.biosystemseng.2016.05.002.

[7] R. Walambe, N. Patwardhan,V. Joshi - "Development of Auto-parking and Collision Avoidance Algorithms on Car type Autonomous Mobile Robots", *IFAC-PapersOnLine* 2020, ISSN 2405-8963, , 53(1), pp. 567-572, https://doi.org/10.1016/j.ifacol.2020.06.095.

[8] B. Yang, W. Luo, R. Urtasun, "PIXOR: Real-Time 3D Object Detection from Point Clouds", *Proceedings of the IEEE Conference on Computer Vision and Pattern Recognition (CVPR)*, June 2018, https://openaccess.thecvf.com/content_cvpr_2018/papers/Yang_PIXOR_Real-Time_3D_CVPR_2018_paper.pdf.

[9] C. Chen, L. Z. Fragonara, A. Tsourdos, "RoIFusion: 3D Object Detection from LiDAR and Vision, Computer Science", ArXiv, 2020, vol. abs/2009.04554, Corpus ID: 221586387.

[10] R. Barea et al., "Vehicle Detection and Localization using 3D LIDAR Point Cloud and Image Semantic Segmentation," 2018 21st International Conference on Intelligent Transportation Systems (ITSC), Maui, HI, USA, 2018, pp. 3481-3486, doi: 10.1109/ITSC.2018.8569962.

[11] L.Ș. Grigore, D. Gorgoteanu, C. Molder, O. Alexa, I. Oncioiu, A. Ștefan, D. Constantin, M. Lupoae and R.I. Bălașa, "A Dynamic Motion Analysis of a Six-Wheel Ground Vehicle for Emergency Intervention Actions," *MDPI-Sensors,* vol. 21, issue 5, 1618, pp. 30, February 2021

[12] X. Wei, J. Li, D. Zhang, K. Feng - "An improved integrated navigation method with enhanced robustness based on factor graph", *Mechanical Systems and Signal Processing* 2021, ISSN 0888-3270, 155, 107565, https://doi.org/10.1016/j.ymssp.2020.107565.

[13] H. Guo, D. Cao, H. Chen, Z. Sun, Y. Hu - "Model predictive path following control for autonomous cars considering a measurable disturbance: Implementation, testing, and verification", Mechanical Systems and Signal Processing 2019, ISSN 0888-3270, 118, pp. 41-60, https://doi.org/10.1016/j.ymssp.2018.08.028.

[14] P.J. Besl and N.D. McKay, "A Method for Registration of 3D Shapes," IEEE Transactions on Pattern Analysis and Machine Intelligence, vol. 14(2): 239-256, 1992.

[15] A. Segal, D. Haehnel, and S. Thrun, "Generalized-ICP," Proceedings of Robotics: Science and Systems, 2009.

[16] C. Forster, L. Carlone, F. Dellaert, and D. Scaramuzza, "On-Manifold Preintegration for Real-Time Visual-Inertial Odometry," IEEE Transactions on Robotics, vol. 33(1): 1-21, 20.

[17] Yu Haige, Yu Fan, Wei Yanxi. "Improved Stereo Vision Robot Locating and Mapping Method", International Journal of Advanced Network, Monitoring and Controls, 2019

[18] T. Shan, B. Englot, D. Meyers, W. Wang, C. Ratti and D. Rus, LIO-SAM: Tightly-coupled Lidar Inertial Odometry via Smoothing and Mapping, 14 July 2020, asXiv: 2007.00258v3 [cs. RO].

[19] T. Ciobotaru, L.Ș. Grigore, V. Vînturiș and others, "Robot for Combating Terrorism ROBTER," Research Project CEEX-2006, Thematic Area 9.1, Protection against terrorism and crime. PT4 technological platform - Advanced engineering materials and technologies, Military Technical Academy, Bucharest.

[20] Cristinel ILIE, Mihai MIHAIESCU, Ionel CHIRITA, Mihai GUTU, Marius POPA, Nicolae TANASE. "Synchronous Electric Generator With Double Excitation", 2019 11th International Symposium on Advanced Topics in Electrical Engineering (ATEE), 2019

Authorized licensed use limited to: Otto-von-Guericke Universitaet Magdeburg. Downloaded on September 11,2022 at 14:08:34 UTC from IEEE Xplore. Restrictions apply.